

## Low-density helium monolayers as two-dimensional imperfect gases: An analysis employing the second virial coefficient\*

R. L. Siddon<sup>†</sup> and M. Schick

*Department of Physics, University of Washington, Seattle, Washington 98195*

(Received 17 September 1973)

The quantum second virial coefficient of two-dimensional systems interacting with a hard-core or Lennard-Jones 6-12 potential are calculated together with the contribution this coefficient makes to the specific heat of such systems. The results are compared with experimental data from low-density He<sup>3</sup> and He<sup>4</sup> monolayers adsorbed on graphite. The calculation provides a qualitative and quantitative understanding of the experimental measurements. In particular it illuminates the manner in which the interaction and the difference in statistics cause the very different specific-heat measurements in the two isotopes. The magnetic susceptibility of low-density He<sup>3</sup> monolayers is predicted.

### I. INTRODUCTION

There has been considerable interest in the recent experiments performed on systems of helium adsorbed on graphite.<sup>1</sup> This interest is merited because such systems are easily prepared over a wide range of densities and temperatures thereby permitting a methodical study of the effects of the interaction, as the system varies from a weakly to a strongly interacting one, and of the quantum mechanics, as it varies from a classical to a highly degenerate state. In addition, the helium behaves as a two-dimensional (2D) system at low temperatures so that a study of the effects of reduced dimensionality upon such phase transitions as solidification<sup>2</sup> and superfluidity<sup>2, 3</sup> can be made. The manner in which these transitions vary with film thickness is also easily investigated.<sup>4</sup>

Heat-capacity-measurement results from high-density monolayer systems of He<sup>3</sup> and He<sup>4</sup> are substantially the same for both isotopes and are qualitatively understood as indicating the existence of solid phases which, depending upon the density, are either in or out of registry with the array of adsorption sites provided by the graphite.<sup>5</sup>

Data from low-density samples, however, have received conflicting interpretations, and the difference in the signals from each isotope has received no satisfactory explanation.

It is the purpose of this paper to show that a study of the virial expansion of the thermodynamic properties of a two-dimensional system of bosons or fermions interacting with a potential appropriate to helium provides a qualitative and quantitative understanding of the experimental data in the low-density regime. In particular, such a study illuminates the manner in which the interparticle interaction and the difference in statistics combine to produce very different signals for the isotopes. The analysis also provides a basis for predictions

relevant to future experiments, such as on the magnetic susceptibility of He<sup>3</sup> films.

In Sec. II we provide a brief review of the heat-capacity data from low-density samples of adsorbed He<sup>3</sup> and He<sup>4</sup>, and indicate those features which we believe need to be understood. Section III is devoted to a formulation of the virial expansion of the thermodynamic properties of a two-dimensional system. In the Sec. IV the formalism is applied to systems interacting with a hard-core or Lennard-Jones 6-12 potential. The results of the latter are compared with experimental data in Sec. V. The possibility of a liquid-gas transition is investigated in Sec. VI. Section VII provides a summary of our understanding of the low-density systems. We conclude with a discussion of the virial expansion of the magnetic susceptibility of He<sup>3</sup> films and a prediction for its behavior at low densities.

### II. REVIEW OF EXPERIMENTAL DATA

We shall examine here the heat-capacity data taken from low-density systems of He<sup>3</sup> and He<sup>4</sup> adsorbed on graphite. In order to give meaning to the term "low density" we note the following. The number densities at which the first helium layer adsorbed on graphite is completed and the second layer begins to form are 0.115 and 0.017 Å<sup>-2</sup> for He<sup>4</sup> and He<sup>3</sup>, respectively. The largest density of any system whose behavior we shall compare with theory is 0.0483 Å<sup>-2</sup>, somewhat less than one-half a monolayer. A lower limit to the densities of interest to us is provided by the observation<sup>6</sup> that inhomogeneities in the graphite substrate make substantial contributions to the heat capacity at densities less than 0.025 Å<sup>-2</sup>.

Figure 1 shows the specific heat for two samples of He<sup>3</sup> of densities 0.0279 (circles) and 0.0415 Å<sup>-2</sup> (plusses) from 1 to 4 K.<sup>7</sup> That the data appear to

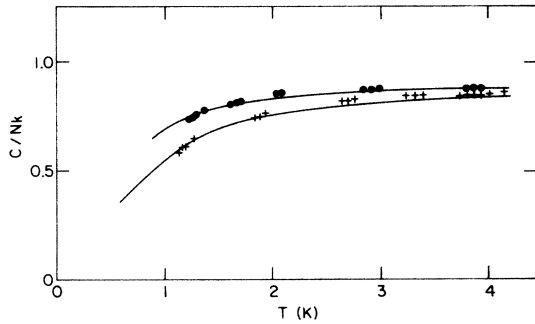


FIG. 1. Specific heats of adsorbed He<sup>3</sup> at densities of 0.0279 (circles) and 0.0415 Å<sup>-2</sup> (pluses).

become asymptotic at high temperatures to a value near unity is evidence for the gaslike nature of the system. The density-dependent deviations from unity are noteworthy as they are much larger than those expected from an ideal Fermi gas. That model yields specific heats which, at 4 K, are within 0.003 and 0.008 of unity for the densities cited above. The solid curves in Fig. 1 are fits to the data made by Bretz and Dash.<sup>7</sup> They used the ideal-Fermi-gas model but accounted for the deviation by assuming that the number of atoms in the gas phase was less than the number of atoms in the system. The Fermi temperatures needed to fit the data, 3.4 and 4.8 K, are in poor agreement with the values calculated from the measured density and bare mass, 1.39 and 2.11 K. As the temperature is lowered, the specific heat continues to fall until about 0.2 K at which temperature a "shoulder" appears as shown<sup>8</sup> in Fig. 2. This feature is very similar to one appearing in bulk He<sup>3</sup> which has been attributed to an ordering of the nuclear spins.<sup>9</sup>

The specific-heat data from He<sup>4</sup> samples are quite different from the above as can be seen from Fig. 3 which shows the signal<sup>7</sup> from He<sup>4</sup> systems

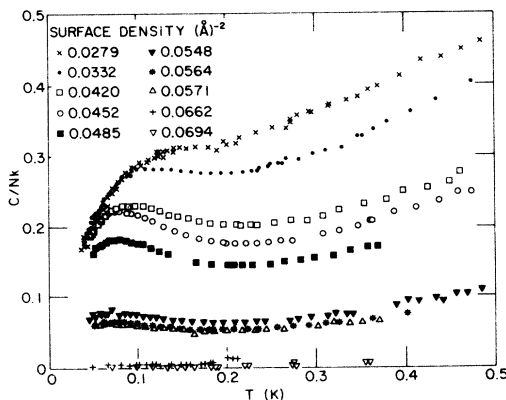


FIG. 2. Low-temperature specific heats of adsorbed He<sup>3</sup> systems.

of densities 0.0273 and 0.0399 Å<sup>-2</sup>. At high temperatures the data become asymptotic to a value near unity indicating a gaslike phase. However there again occurs a significant density-dependent deviation from unity. By comparing the 0.0273 Å<sup>-2</sup> signal of Fig. 3 with that of the 0.0279 Å<sup>-2</sup> He<sup>3</sup> signal in Fig. 1, it is seen that for the same density, the He<sup>3</sup> signal shows a greater deviation from unity. As the temperature is lowered, the He<sup>4</sup> data rise. We note that the curves cross one another at 2.2 K. Finally, they reach a maximum and begin to fall. This signal has been variously interpreted as indicating the presence of long-range inhomogeneities in the graphite<sup>10</sup> or a liquid-gas transition.<sup>11</sup> It is natural to enquire whether any of the features of the heat-capacity signals can be attributed to the band structure induced by the periodic substrate potential. This structure has been calculated by Hagen, Milford, and Novaco.<sup>12</sup> They find that for energies within 70 K of the bottom of the lowest band, the band structure is little changed from that of a free particle. The small changes which do occur consist of the introduction of narrow band gaps and the splitting of degeneracies. Assuming that the He atoms interact *only* with the substrate, Hagen *et al.* calculate the specific heat of the system. Because the effects of the periodic potential on the bands is small, the heat capacity resembles that of an ideal gas with small deviations. Of interest to us is the fact that the specific heat is reduced by about 10% of the ideal value at 4 K, so that the deviation from unity observed in the data might be attributable to the band structure. The effect of the assumption of zero interparticle interaction is unknown however. Further, the specific heat of ideal bosons and spin- $\frac{1}{2}$  fermions are very similar (they would be identical in 2D if the two systems had the same spin<sup>13</sup>) so that the band structure, which produces only small differences from the ideal results, cannot account for the dif-

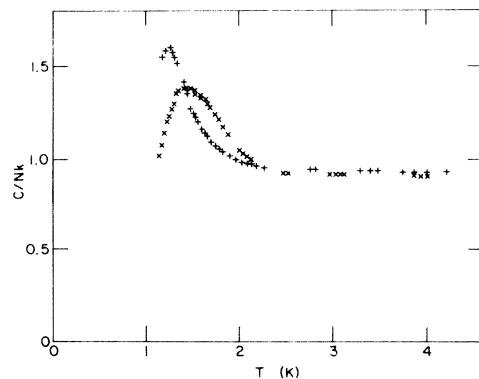


FIG. 3. Specific heats of adsorbed He<sup>4</sup> at densities of 0.0273 (pluses) and 0.0399 Å<sup>-2</sup> (crosses).

ferences in the experimental signals.

We are therefore led to an investigation of the effects of the two-particle interaction in order to explicate the significant features of the experimental specific-heat signals which, for the reader's convenience, we summarize below.

(i) At 4 K the specific heat of both isotopes is significantly less than unity with greater deviations occurring for samples of greater density. For equal densities, the signal from He<sup>3</sup> deviates more than that of He<sup>4</sup>.

(ii) With decreasing temperature the He<sup>4</sup> signals rise and cross one another at about 2 K. They reach a peak at about 1.5 K and then fall.

(iii) With decreasing temperature the He<sup>3</sup> signals fall. Near 0.2 K a "shoulder" in the signal appears.

### III. THEORY

#### A. Virial expansion

The problem of the interacting classical gas with pair interactions was first put into tractable form by means of a cluster-expansion technique developed by Ursell and Mayer.<sup>14</sup> Their method was subsequently generalized by Kahn and Uhlenbeck<sup>15</sup> who introduced a cluster-expansion formalism, valid for classical or quantum-mechanical systems with a general interaction potential. Another method was later developed by Kilpatrick.<sup>16</sup> His procedure is described as follows.

The definition of the grand partition function is

$$\mathcal{Q}(z, A, T) = \sum_{l=0}^{\infty} Z_l(A, T) z^l, \quad (3.1)$$

where  $Z_l(A, T)$  is the canonical partition function for  $l$  particles and  $z$  is the fugacity. If the logarithm of the grand partition function is expanded in a power series in  $z$ , called the cluster expansion,

$$\frac{1}{A} \ln \mathcal{Q}(z, A, T) = \sum_{l=1}^{\infty} b_l(A, T) z^l, \quad (3.2)$$

then the coefficient  $b_l(A, T)$ , called the  $l$ th cluster integral, can be found by comparing the series expansion of  $\exp[\ln \mathcal{Q}(z, A, T)]$  with Eq. (3.1). The procedure is straightforward and the result is

$$b_l(A, T) = \frac{1}{A} \sum_{\{m\}} (-1)^{\delta-1} (\delta-1)! \prod_{j=1}^l Z_j^{m_j}(A, T) / m_j!, \quad (3.3)$$

where  $\delta \equiv \sum_{j=1}^l m_j$ , and the summation is over all sets of positive integers  $m_j$  including zero such that  $\sum_{j=1}^l j m_j = l$ .

The expansion of the logarithm of the grand par-

tition function, Eq. (3.2), with  $b_l(A, T)$  given by Eq. (3.3) is the principal result of the cluster-expansion technique. The thermodynamic functions of the system are found by eliminating the quantity  $z$  from the parametric equations of state for the spreading pressure

$$\beta \varphi = \frac{1}{A} \ln \mathcal{Q}(z, A, T) = \sum_{l=1}^{\infty} b_l(A, T) z^l, \quad (3.4)$$

with  $\beta = 1/kT$ , and particle density

$$n = \frac{1}{A} z \frac{\partial}{\partial z} \ln \mathcal{Q}(z, A, T) = \sum_{l=1}^{\infty} l b_l(A, T) z^l. \quad (3.5)$$

In particular, eliminating  $z$  by expressing the pressure in a power series in the density yields the so-called virial expansion of the equation of state,

$$\beta \varphi = \sum_{l=1}^{\infty} B_l(A, T) n^l, \quad (3.6)$$

where  $B_l(A, T)$  is called the  $l$ th virial coefficient. The first virial coefficient is identically unity. If the density, given by Eq. (3.5), is substituted into the virial expansion and the resulting expression compared with Eq. (3.4), then the virial coefficient can be found by solving in succession the system of equations

$$b_l(A, T) = \sum_{\{m\}} B_{\delta}(A, T) \delta! \times \prod_{j=1}^l [j b_j(A, T)]^{m_j} / m_j!. \quad (3.7)$$

The virial coefficients are given in terms of the partition functions by eliminating the cluster integrals in the above expression, using Eq. (3.3).

In the thermodynamic limit, the area and number of particles of the system become infinite while the density  $N/A$  remains finite. As this is the case of interest, the virial coefficient is redefined by

$$B_l(T) = \lim_{A \rightarrow \infty} B_l(A, T),$$

and is assumed to exist in the limit.

It follows from the expansion of the pressure, Eq. (3.6), together with the fact that in the limit of zero density all thermodynamic functions must reduce to their noninteracting classical values (denoted below by the subscript zero), that for the interacting system, the Helmholtz free energy is

$$\beta F/N = \beta F_0/N + \sum_{l=1}^{\infty} l^{-1} B_{l+1}(T) n^l.$$

The other thermodynamic functions can be found

from this result. Of particular interest to us is the specific heat at constant area:

$$\frac{C}{Nk} = \frac{C_0}{Nk} - \beta^2 \frac{d^2}{d\beta^2} \sum_{i=1}^{\infty} B_{i+1}(T) \frac{n^i}{l}. \quad (3.8)$$

The presence of the substrate greatly complicates the calculation of the virial coefficients. In order to make our problem tractable we shall henceforth ignore the periodic potential due to the substrate. The substrate potential appears only implicitly in that we treat the adsorbed helium as a 2D system.

With the above assumptions

$$F_0 = N\beta^{-1} \{ \ln[n\lambda^2/(2s+1)] - 1 \}, \quad C_0 = Nk, \quad (3.9)$$

where  $\lambda \equiv (2\pi\hbar^2\beta/M)^{1/2}$  is the thermal wavelength, and  $s$  is the spin of the particle.

The  $l$ th virial coefficient, being related to the  $l$ -particle partition function, requires the solution of the  $l$ -body problem. For most problems therefore, expansions of the thermodynamic quantities are truncated after the second virial coefficient.<sup>17</sup> In particular, the specific heat becomes

$$\frac{C}{Nk} = 1 - n\beta^2 \frac{d^2 B_2(T)}{d\beta^2}, \quad (3.10)$$

where Eq. (3.9) has been used. The range of temperature and density for which this expression is adequate must be investigated.

### B. Second virial coefficient

The second virial coefficient, henceforth denoted  $B(\beta)$ , can, from Eqs. (3.3) and (3.7), be written in the form

$$B(\beta) = - \lim_{A \rightarrow \infty} A [ Z_2(A, \beta) - \frac{1}{2} Z_1^2(A, \beta) ] / Z_1^2(A, \beta). \quad (3.11)$$

For purposes of orientation, it should be noted that, from the expansion of the virial equation of state [Eq. (3.6)]

$$\beta\phi/n = 1 + nB + \dots$$

$B$  is expected to be positive for repulsive potentials thereby causing an increase in the pressure over its ideal-gas value, and negative for attractive potentials, causing a decrease in the pressure.

For potentials which only depend on the magnitude of the relative separation between particles, and the potentials with which we are concerned are of this kind, the following classical expression is easily obtained from Eq. (3.10):

$$B(\beta) = \frac{1}{2} \int_0^{\infty} (1 - e^{-\beta V(r)}) 2\pi r dr.$$

Substituting this classical approximation into Eq.

(3.10), one obtains

$$C/Nk - 1 = n\beta^2 \int_0^{\infty} V(r)^2 e^{-\beta V(r)} 2\pi r dr.$$

We observe that, in the classical approximation, the deviation of the specific heat from unity is always positive. However, it was noted that the observed deviations of the specific heat of the helium monolayers are negative. As the classical approximation can not explain these deviations or the He<sup>3</sup> specific heat, it is necessary to turn to the quantum-mechanical expression for the second virial coefficient.

The quantum-mechanical partition function for  $N$  identical particles is

$$Z_N(A, \beta) = \int d\vec{r}_1 \cdots d\vec{r}_N \sum_{\alpha} \psi_{\alpha}^*(\vec{r}_N) \times e^{-\beta H(\vec{p}_N, \vec{r}_N)} \psi_{\alpha}(\vec{r}_N), \quad (3.12)$$

where the  $\psi_{\alpha}(\vec{r}_N)$  are any complete orthonormal set of wave functions. For bosons (fermions) the summation is only over those states which are totally symmetric (antisymmetric) under exchange of particle coordinates, including spin. As the spin dependence of our problem is trivial, we consider first spinless particles and insert the appropriate spin factors at the end of the development. As the single-particle partition function  $Z_1(A, T)$  is simply  $A/\lambda^2$ , the second virial coefficient for spinless particles is, from Eqs. (3.11) and (3.12),

$$B(\beta) = \lim_{A \rightarrow \infty} \frac{1}{2A} \iint \left( 1 - 2\lambda^4 \sum_{\alpha} \psi_{\alpha}^*(\vec{r}_1, \vec{r}_2) \times e^{-\beta H} \psi_{\alpha}(\vec{r}_1, \vec{r}_2) \right) d\vec{r}_1 d\vec{r}_2.$$

For convenience, the wave functions  $\psi_{\alpha}$  are taken to be eigenfunctions of the two-body Hamiltonian with eigenvalues  $E_{\alpha}$ . As usual,  $\psi_{\alpha}$  can be factored into a center-of-mass wave function multiplied by the relative wave function. Upon carrying out the sum over all center-of-mass momenta, the expression for  $B(\beta)$  becomes

$$B(\beta) = \lim_{A \rightarrow \infty} \frac{1}{2} \int \left( 1 - 4\lambda^2 \sum_n |\psi_n(\vec{r})|^2 e^{-\beta E_n} \right) d\vec{r}, \quad (3.13)$$

where  $\psi_n$  and  $E_n$  are the relative eigenfunctions and eigenvalues. In the absence of any two-body potential, the virial coefficient is given by its ideal value  $B^0(\beta)$ , where

$$B^0(\beta) = \lim_{A \rightarrow \infty} \frac{1}{2} \int \left( 1 - 4\lambda^2 \sum_n |\psi_n^0(\vec{r})|^2 e^{-\beta E_n^0} \right) d\vec{r}. \quad (3.14)$$

Using properly symmetrized plane waves, one can easily evaluate this expression and obtain

$$B^0(\beta) = \mp \frac{1}{4} \lambda^2, \quad (3.15)$$

where the minus sign is for bosons and reflects the statistical attraction which decreases the pressure from its classical ideal value. Similarly the positive sign for fermions is due to the statistical repulsion.

By subtracting Eqs. (3.13) and (3.14) and using the fact that the relative wave functions are normalized, the second virial coefficient can be written

$$B(\beta) = B^0(\beta) + \lim_{A \rightarrow \infty} 2\lambda^2 \sum_n (e^{-\beta E_n^0} - e^{-\beta E_n}). \quad (3.16)$$

Because of the cylindrical symmetry of the potential the relative quantum numbers can be taken to be the usual azimuthal quantum number  $m$  and a radial quantum number  $k$  which is related to the relative energy according to

$$E_k = \hbar^2 k^2 / 2\mu,$$

where  $\mu$  is the reduced mass. The resulting sums over the azimuthal quantum number contain only even values of  $m$  ( $0, \pm 2, \pm 4, \dots$ ) for bosons and odd values of  $m$  ( $\pm 1, \pm 3, \dots$ ) for fermions. Equation (3.16) is further simplified by writing the sum over any bound states of the potential explicitly and replacing the sum over the quasicontinuum of states by an integration weighted with a density of states. The resulting expression is

$$B(\beta) = B^0(\beta) - 2\lambda^2 \sum_B' e^{-\beta E_B} - 2\lambda^2 \int_0^\infty \sum' [g_m(k) - g_m^0(k)] e^{-\beta \hbar^2 k^2 / 2\mu} dk, \quad (3.17)$$

where the subscript  $B$  stands for bound states and prime on the sum denotes a restriction to even or odd values of  $m$ .

The difference in density of states is usually related to the scattering phase shifts by the following argument.<sup>18</sup> The relative wave function  $\psi_{m,k}(r)$  can be factored into a product of a trivial azimuthal part and nontrivial radial wave functions  $R_{m,k}(r)$  which satisfies the equation

$$\frac{1}{r} \frac{d}{dr} \left( r \frac{d}{dr} R_{m,k}(r) \right) + (k^2 - m^2/r^2) R_{m,k}(r) = [2\mu V(r)/\hbar^2] R_{m,k}(r). \quad (3.18)$$

For large value of  $r$  where the potential is assumed negligible,

$$R_{m,k}(r) \sim \cos[kr - \frac{1}{4}\pi - \frac{1}{2}m\pi + \delta_m(k)], \quad (3.19)$$

which defines the phase shift  $\delta_m(k)$  of the  $m$ th partial wave. If the system is placed within a cylinder of radius  $R$ , the vanishing of the wave function at the boundary requires, for the noninteracting system, that

$$\cos(kR - \frac{1}{4}\pi - \frac{1}{2}m\pi) = 0,$$

so that the allowed values of  $k$  are given by

$$kR - \frac{1}{4}\pi - \frac{1}{2}m\pi = (n + \frac{1}{2})\pi, \quad n = 0, 1, 2, \dots$$

The change in  $k$ ,  $\Delta k$ , with a change in  $n$ ,  $\Delta n = 1$ , is easily obtained from the above as is  $g^0(k)$  which is the limit of  $\Delta n / \Delta k$  as  $R$  becomes infinite and  $\Delta k$  vanishes. One obtains

$$g_m^0(k) = R/\pi.$$

The same argument applied to the interacting system yields

$$kR - \frac{1}{4}\pi - \frac{1}{2}m\pi + \delta_m(k) = (n + \frac{1}{2})\pi$$

and

$$g_m(k) = \frac{1}{\pi} \left( R + \frac{\partial \delta_m(k)}{\partial k} \right),$$

so that

$$g_m(k) - g_m^0(k) = \frac{1}{\pi} \frac{\partial \delta_m(k)}{\partial k},$$

which is the quantity which appears in Eq. (3.17). The above expression is substituted into Eq. (3.17) and a partial integration is carried out. Using the fact<sup>19</sup> that the number of bound states with azimuthal quantum number  $m$  is equal to  $\delta_m(0)/\pi$ , we obtain the final expression for the second virial coefficient of a spinless Bose or Fermi system:

$$B(\beta) = \mp \frac{1}{4} \lambda^2 - 2\lambda^2 \sum_B' (e^{-\beta E_B} - 1) - \frac{2\lambda^4}{\pi^2} \int_0^\infty dk k \sum_m' \delta_m(k) e^{-\beta \hbar^2 k^2 / 2\mu}. \quad (3.20)$$

The origin of the first, ideal, term has already been discussed. Since  $E_B$  is negative, the contribution of the second term, which reflects the possibility of forming bound pairs, is negative. Thus, this possibility causes a decrease in the pressure as expected. That the last term, which contains all other effects of the interaction, has the correct sign is seen when it is recalled that the phase shifts of repulsive potentials are negative and those of attractive potentials are positive. Thus this term is positive for repulsive potentials and negative for attractive potentials as expected.

The virial coefficient for a system of spin  $s$  can

now be related to those for spinless Bose and Fermi systems. There are  $(2s+1)^2$  spin states of which a fraction  $(s+1)/(2s+1)$  are symmetric and  $s/(2s+1)$  are antisymmetric. For a fermion system, the symmetric spin states must be multiplied by antisymmetric spatial states which enter into the spinless-fermion virial coefficient  $B_F(\beta)$ . Similarly the antisymmetric spin states multiply symmetric spatial states which enter into the spinless-boson virial coefficient  $B_B(\beta)$ . Thus

$$B_F^{(s)}(\beta) = \frac{s+1}{2s+1} B_F(\beta) + \frac{s}{2s+1} B_B(\beta).$$

In particular, for spin- $\frac{1}{2}$  fermions

$$B_F^{(1/2)}(\beta) = \frac{3}{4} B_F(\beta) + \frac{1}{4} B_B(\beta). \quad (3.21)$$

A similar argument for bosons yields

$$B_B^{(s)}(\beta) = \frac{s+1}{2s+1} B_B(\beta) + \frac{s}{2s+1} B_F(\beta).$$

Lastly we state without proof that the second virial coefficient of a binary mixture of components  $C$  and  $D$  having second virial coefficients  $B_C^{(s)}$ ,  $B_D^{(s')}$  and densities  $n_C$ ,  $n_D$ , respectively, is<sup>20</sup>

$$B(\beta) = \left(\frac{n_C}{n}\right)^2 B_C^{(s)} + \left(\frac{n_C n_D}{n^2}\right) B_{CD} + \left(\frac{n_D}{n}\right)^2 B_D^{(s')},$$

where

$$n = n_C + n_D,$$

and  $B_{CD}$  can be put in the form

$$B_{CD} = -\lambda_\mu^2 \sum_B (e^{-\beta E_B} - 1) - (\lambda_\mu/\pi)^2 \int_0^\infty dk k \sum_m \delta_m(k) e^{-\beta \hbar^2 k^2 / 2\mu}. \quad (3.22)$$

In this expression  $E_B$  and  $\delta_m(k)$  are the bound states and phase shifts of the two-particle (one  $C$ , one  $D$ ) problem, the sum is over all values of  $m$  and

$$\lambda_\mu^2 = 2\pi\hbar^2\beta/2\mu,$$

$$\mu = M_C M_D / (M_C + M_D).$$

It is easily shown that  $B_{CD}$  is simply the second virial coefficient of a system of distinguishable particles of mass  $2\mu$ .

In Sec. IV we calculate the phase shifts, second virial coefficient, and the contribution to the specific heat from two interactions of interest to us: the hard-core and Lennard-Jones 6-12 potentials.

#### IV. APPLICATION OF THEORY

##### A. Hard-core interaction

We choose to study first the infinitely repulsive hard-core potential [ $V(r)$  is infinite for  $r < a$  and

vanishes otherwise] because any realistic helium interaction will contain a strong short-range repulsion. The effects of this repulsion can more easily be separated from the effects of an additional weak attraction by examining a simple case which consists solely of repulsion.

The solution of the radial equation, Eq. (3.18), for  $r$  greater than  $a$  is

$$R_{m,k}(r) = C_m(k) [J_m(kr) \cos \delta_m(k) - Y_m(kr) \sin \delta_m(k)],$$

where  $\delta_m(k)$  is the phase shift defined previously by Eq. (3.19), and  $J_m(kr)$ ,  $Y_m(kr)$  are the cylindrical Bessel functions of order  $m$  of the first and second kind, respectively. The condition that the relative wave function vanishes at  $r$  equal to  $a$ , determines the phase-shift modulo  $\pi$  according to

$$\tan \delta_m(q) = J_m(q)/Y_m(q), \quad (4.1)$$

where  $q \equiv ka$ .

Since  $\delta_m(0)$  is equal to the number of bound states with azimuthal quantum number  $m$  and the hard-core potential has no bound states, we know that  $\delta_m(0)$  vanishes. The absolute value of the phase shift at any other value of  $q$  can then be obtained by requiring that  $\delta_m(q)$  be a continuous function of  $q$ .

These phase shifts are used to calculate the second virial coefficient according to Eq. (3.20). The third term in that equation was evaluated numerically. For a given value of  $k$ , the phase-shift sum included all even or odd values of  $m$  whose absolute value was less than some integer  $\nu$  which was determined by the condition

$$\delta_\nu(q) \leq 10^{-5} \text{ rad.}$$

The integral over  $k$  was evaluated numerically with the upper limit replaced by a large value of  $k$  determined as follows. The error made in truncating the integral depends on the asymptotic form of the phase-shift sum for large  $k$ . This form is found by noting that

$$\begin{aligned} \frac{d}{dq} \tan \delta_m(q) &= \frac{d\delta_m(q)}{dq} \frac{1}{\cos^2 \delta_m(q)} \\ &= \frac{d\delta_m(q)}{dq} \frac{[Y_m^2(q) + J_m^2(q)]}{Y_m^2(q)}, \end{aligned}$$

using Eq. (4.1). However, differentiating this equation directly yields

$$\frac{d}{dq} \tan \delta_m(q) = -\frac{2}{\pi q Y_m^2(q)}.$$

Therefore

$$\sum_{m=-\infty}^{\infty} \frac{d\delta_m(q)}{dq} = -\frac{2}{\pi q} \sum_{m=-\infty}^{\infty} \frac{1}{J_m^2(q) + Y_m^2(q)}.$$

TABLE I. Second virial coefficients for two-dimensional hard-core fermions.

$T^\star$	$B^\star$	$\beta \frac{dB^\star}{d\beta}$	$\beta^2 \frac{d^2B^\star}{d\beta^2}$
0.500 00	4.756 13	2.510 97	-0.549 23
1.000 00	3.400 62	1.503 55	-0.445 24
1.500 00	2.869 19	1.137 39	-0.370 22
2.000 00	2.571 54	0.938 99	-0.320 60
2.500 00	2.376 60	0.811 67	-0.286 01
3.000 00	2.236 99	0.721 83	-0.260 45
3.500 00	2.131 00	0.654 45	-0.240 65
4.000 00	2.047 19	0.601 70	-0.224 75
4.500 00	1.978 87	0.559 06	-0.211 63
5.000 00	1.921 84	0.523 75	-0.200 55
5.500 00	1.873 36	0.493 93	-0.191 05
6.000 00	1.831 51	0.468 33	-0.182 78
6.500 00	1.794 92	0.446 08	-0.175 49
7.000 00	1.762 59	0.426 52	-0.169 01
7.500 00	1.733 77	0.409 15	-0.163 19
8.000 00	1.707 87	0.393 61	-0.157 94
8.500 00	1.684 43	0.379 61	-0.153 16
9.000 00	1.663 10	0.366 91	-0.148 79
9.500 00	1.643 58	0.355 32	-0.144 78
10.000 00	1.625 63	0.344 70	-0.141 07
10.500 00	1.609 05	0.334 92	-0.137 63
11.000 00	1.593 68	0.325 88	-0.134 43
11.500 00	1.579 38	0.317 49	-0.131 45
12.000 00	1.566 04	0.309 68	-0.128 65
12.500 00	1.553 54	0.302 38	-0.126 03
13.000 00	1.541 82	0.295 55	-0.123 56
13.500 00	1.530 79	0.289 14	-0.121 23
14.000 00	1.520 38	0.283 10	-0.119 02
14.500 00	1.510 55	0.277 41	-0.116 94
15.000 00	1.501 23	0.272 03	-0.114 95
15.500 00	1.492 40	0.266 93	-0.113 07
16.000 00	1.484 00	0.262 09	-0.111 27
16.500 00	1.476 01	0.257 50	-0.109 56
17.000 00	1.468 39	0.253 12	-0.107 93
17.500 00	1.461 11	0.248 95	-0.106 36
18.000 00	1.454 15	0.244 97	-0.104 87
18.500 00	1.447 49	0.241 16	-0.103 43
19.000 00	1.441 11	0.237 52	-0.102 06
19.500 00	1.434 99	0.234 03	-0.100 73
20.000 00	1.429 10	0.230 68	-0.099 46
20.500 00	1.423 45	0.227 46	-0.098 25
21.000 00	1.418 00	0.224 37	-0.097 07
21.500 00	1.412 76	0.221 40	-0.095 95
22.000 00	1.407 70	0.218 54	-0.094 87
22.500 00	1.402 82	0.215 78	-0.093 84
23.000 00	1.398 11	0.213 12	-0.092 85
23.500 00	1.393 55	0.210 55	-0.091 90
24.000 00	1.389 15	0.208 07	-0.091 01
24.500 00	1.384 88	0.205 67	-0.090 16
25.000 00	1.380 75	0.203 35	-0.089 36
25.500 00	1.376 74	0.201 11	-0.088 62
26.000 00	1.372 86	0.198 94	-0.087 93
26.500 00	1.369 09	0.196 84	-0.087 30
27.000 00	1.365 43	0.194 80	-0.086 74
27.500 00	1.361 87	0.192 83	-0.086 24
28.000 00	1.358 42	0.190 93	-0.085 82
28.500 00	1.355 05	0.189 08	-0.085 48
29.000 00	1.351 78	0.187 29	-0.085 23
29.500 00	1.348 59	0.185 56	-0.085 06
30.000 00	1.345 49	0.183 88	-0.085 00

TABLE II. Second virial coefficients for two-dimensional hard-core bosons.

$T^\star$	$B^\star$	$\beta \frac{dB^\star}{d\beta}$	$\beta^2 \frac{d^2B^\star}{d\beta^2}$
0.500 00	4.723 74	2.395 31	-0.784 22
1.000 00	3.399 16	1.495 12	-0.476 84
1.500 00	2.869 15	1.136 59	-0.375 34
2.000 00	2.571 59	0.938 98	-0.321 44
2.500 00	2.376 64	0.811 73	-0.286 11
3.000 00	2.237 01	0.721 89	-0.260 43
3.500 00	2.131 02	0.654 49	-0.240 61
4.000 00	2.047 21	0.601 73	-0.224 72
4.500 00	1.978 88	0.559 09	-0.211 60
5.000 00	1.921 85	0.523 77	-0.200 53
5.500 00	1.873 37	0.493 94	-0.191 03
6.000 00	1.831 52	0.468 35	-0.182 76
6.500 00	1.794 93	0.446 10	-0.175 48
7.000 00	1.762 60	0.426 53	-0.169 00
7.500 00	1.733 77	0.409 16	-0.163 18
8.000 00	1.707 87	0.393 62	-0.157 93
8.500 00	1.684 44	0.379 62	-0.153 15
9.000 00	1.663 10	0.366 91	-0.148 79
9.500 00	1.643 58	0.355 32	-0.144 77
10.000 00	1.625 63	0.344 70	-0.141 06
10.500 00	1.609 05	0.334 92	-0.137 63
11.000 00	1.593 68	0.325 88	-0.134 43
11.500 00	1.579 38	0.317 49	-0.131 44
12.000 00	1.566 04	0.309 68	-0.128 65
12.500 00	1.553 55	0.302 39	-0.126 02
13.000 00	1.541 82	0.295 56	-0.123 55
13.500 00	1.530 79	0.289 14	-0.121 22
14.000 00	1.520 38	0.283 10	-0.119 02
14.500 00	1.510 55	0.277 41	-0.116 93
15.000 00	1.501 24	0.272 03	-0.114 95
15.500 00	1.492 40	0.266 93	-0.113 07
16.000 00	1.484 00	0.262 09	-0.111 27
16.500 00	1.476 01	0.257 50	-0.109 56
17.000 00	1.468 39	0.253 12	-0.107 93
17.500 00	1.461 11	0.248 95	-0.106 36
18.000 00	1.454 15	0.244 97	-0.104 87
18.500 00	1.447 49	0.241 16	-0.103 43
19.000 00	1.441 11	0.237 52	-0.102 05
19.500 00	1.434 99	0.234 03	-0.100 73
20.000 00	1.429 10	0.230 68	-0.099 46
20.500 00	1.423 45	0.227 47	-0.098 24
21.000 00	1.418 00	0.224 38	-0.097 07
21.500 00	1.412 76	0.221 40	-0.095 95
22.000 00	1.407 70	0.218 54	-0.094 87
22.500 00	1.402 82	0.215 78	-0.093 84
23.000 00	1.398 11	0.213 12	-0.092 85
23.500 00	1.393 55	0.210 55	-0.091 90
24.000 00	1.389 15	0.208 07	-0.091 01
24.500 00	1.384 88	0.205 67	-0.090 16
25.000 00	1.380 75	0.203 35	-0.089 36
25.500 00	1.376 74	0.201 11	-0.088 62
26.000 00	1.372 86	0.198 94	-0.087 93
26.500 00	1.369 09	0.196 84	-0.087 31
27.000 00	1.365 43	0.194 80	-0.086 74
27.500 00	1.361 87	0.192 83	-0.086 25
28.000 00	1.358 42	0.190 93	-0.085 83
28.500 00	1.355 05	0.189 08	-0.085 49
29.000 00	1.351 78	0.187 29	-0.085 24
29.500 00	1.348 59	0.185 56	-0.085 08
30.000 00	1.345 49	0.183 89	-0.085 01

The asymptotic form of this sum for large  $q$  is<sup>21</sup>  $(\frac{1}{2}\pi q)^2$ . If this result is substituted into the above and the resulting equation is integrated, one finds

$$\lim_{q \rightarrow \infty} \sum_{m=-\infty}^{\infty} \delta_m(q) = -\frac{1}{4} \pi q^2.$$

The limit of the sum over even or odd values is just  $\frac{1}{2}$  of this. When this asymptotic dependence is used in Eq. (3.20), it is seen that the error made in the dimensionless quantity  $B(\beta)/a^2$ , upon truncating the integral at a value  $k_c \equiv q_c/a$  is of order

$$\int_{q_c^2/T^*}^{\infty} x e^{-x} dx = e^{-q_c^2/T^*} (q_c^2/T^* + 1),$$

where  $T^* \equiv kTM a^2/\hbar^2$  and  $M$  is the particle mass. A cut off of  $q_c = 20$  was used for  $T^*$  up to 30. From the above, the error in  $B(\beta)/a^2$  is of the order of  $2 \times 10^{-5}$ . It is convenient to measure  $B(\beta)$  in units of its classical value, which, from Eq. (3.11) is simply  $\frac{1}{2}\pi a^2$ . We therefore define

$$B^* \equiv 2B/\pi a^2.$$

A tabulation of  $B^*$  versus  $T^*$  appears in Tables I and II. These values are in good agreement with those calculated by Steele and Derderian.<sup>22</sup> The results are shown graphically in Fig. 4. There are at least two interesting features. First, the virial coefficient is substantially larger than its classical value even out to  $T^*$  of 30. Second, the effects of statistics is negligible for  $T^*$  greater than about one. The reason for this is well understood and has been investigated in detail by Boyd, Larsen, and Kilpatrick.<sup>23</sup> The essence of the argument is that exchange effects are only important

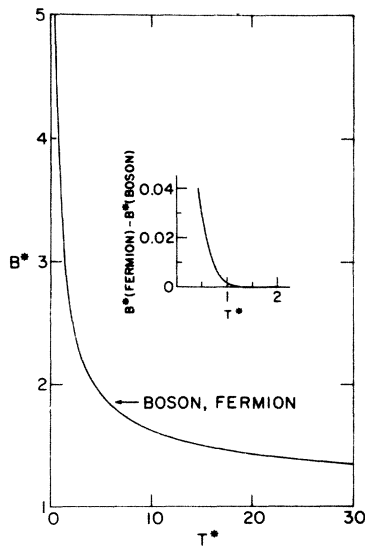


FIG. 4. Second virial coefficients for 2D hard-core systems.

when the particles are within a thermal wavelength of one another. This is impossible when the thermal wavelengths are smaller than the hard-core diameter and this condition occurs for  $T^*$  greater than or on the order of unity. It will be seen later that this suppression of exchange effects by the potential will be important in the interpretation of our results for the susceptibility of He<sup>3</sup>.

The contribution of the second virial coefficient to the specific heat,

$$-\beta^2 \frac{d^2 B^*}{d\beta^2} \approx 2 \frac{C/Nk - 1}{n\pi a^2},$$

was obtained by performing the differentiations with respect to  $\beta$  on Eq. (3.20) and evaluating the resulting expression numerically. The results for this quantity, as well as those for  $\beta dB^*/d\beta$  which enters the virial expansion of the entropy, are presented in Tables I and II. Figure 5 shows the quantity  $-\beta^2 d^2 B^*/d\beta^2$  vs  $T^*$ . From this figure it can be seen that the specific heats for both bosons and fermions are essentially identical above  $T^*$  of unity and that  $C/Nk$  is greater than unity. With decreasing temperature, the specific heats increase. Ultimately the specific heat of the quantum-mechanical system must fall to zero but this decrease is not contained in the second virial coefficient. It can be stated from the above results, however, that at low densities, the specific heat of hard-core boson or fermion systems will have a rounded peak. This behavior is similar to the experimental signals from He<sup>4</sup> films and gives a clue as to its origin. However the analysis of the hard-core systems sheds no light on the negative deviation of the heat capacity at high temperatures or the great difference between the He<sup>3</sup> and He<sup>4</sup> signals.

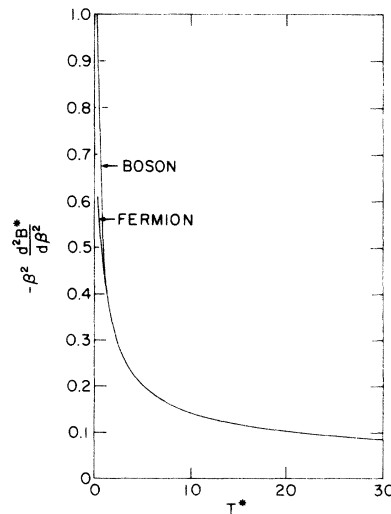


FIG. 5. Deviation of the specific heat from unity per unit density for a hard-core system.

We can only hope that a more realistic potential will elucidate these features and therefore turn to the Lennard-Jones potential.

### B. Lennard-Jones 6-12 potential

The Lennard-Jones 6-12 potential defined by

$$V(r) = 4\epsilon[(\sigma/r)^{12} - (\sigma/r)^6] \quad (4.2)$$

is very often used to represent the interaction between two inert atoms. Approximation methods have been employed to calculate the second virial coefficient of a 2D system interacting with such a potential,<sup>22</sup> but we believed that these methods yield inaccurate results in the temperature range of primary interest to us.<sup>24</sup> We have therefore applied the procedure outlined in the Sec. IV A to the above potential.

The solution of the radial Schrödinger equation containing the Lennard-Jones potential are not common tabulated functions and must therefore be calculated numerically. The Schrödinger equation was integrated using the Numerov process<sup>25</sup> for given values of  $q = k\sigma$  and  $m$ . By starting the integration well within the repulsive part of the potential, the solution becomes independent of the precise starting values. The integration is carried out to a cut off  $r_c$  and the phase shift is determined modulo  $\pi$  from the usual matching condition which gives

$$\tan\delta_m(q) = \frac{qR_{m,q}(x_c)J'_m(qx_c) - J_m(qx_c)R'_{m,q}(x_c)}{qR_{m,q}(x_c)Y'_m(qx_c) - Y_m(qx_c)R'_{m,q}(x_c)}, \quad (4.3)$$

where  $x \equiv r/\sigma$  and the prime denotes a derivative with respect to the argument. Once the number of bound states is known, the absolute value of the phase shift can be found as outlined in the discussion of the hard-core problem. It was desired that the cut off be chosen so that the contribution to the phase shift of that part of the potential beyond the cut off was less than  $10^{-5}$  rad. It can be shown<sup>20</sup> that this requires that, for a given  $q$ ,

$$x_c \geq 10(p^2/5q)^{1/5},$$

where

$$p^2 \equiv 8\mu\epsilon\sigma^2/\hbar^2.$$

For sufficiently large values of  $|m|$ , the phase shifts approach those given by the Born approximation

$$\delta_m^{\text{Born}} = -(\mu\pi/\hbar^2) \int_0^\infty V(r)J_m^2(kr) dr,$$

which for the Lennard-Jones potential are given by

$$\delta_m^{\text{Born}} = -\frac{\pi p^2 q^{10}}{2^{12}} \frac{\Gamma(11)\Gamma(|m|-5)}{\Gamma^2(6)\Gamma(|m|+6)} + \frac{\pi p^2 q^4}{2^6} \frac{\Gamma(5)\Gamma(|m|-2)}{\Gamma^2(3)\Gamma(|m|+3)}, \quad |m| > 5.$$

The phase-shift sums were obtained by summing the results from the numerical routine until the Born approximation was accurate to within  $10^{-5}$  rad. The Born phase shifts were then summed until the contribution from the largest  $|m|$  was less than  $10^{-5}$  rad. The error in the phase-shift sum, for a particular value of  $q$ , due to all effects, is estimated to be less than  $4 \times 10^{-4}$  rad. The phase-shift sums were calculated for values of  $q$  from 0.1 to 20.0 in steps of 0.1. The integral appearing in Eq. (3.20) for the second virial coefficient was computed using a cut off in the range of integration of  $q_c = 20$ . To determine the error caused by this truncation the asymptotic form of the phase shift sum for large  $q$  must be obtained. This was done by comparing the quantum-mechanical expression for the second virial coefficient of a gas of distinguishable particles, given by Eq. (3.22), with the classical expression which, for the Lennard-Jones 6-12 potential, is

$$B_{CL} = -\pi\sigma^2 \sum_{j=0}^{\infty} \frac{1}{12j!} (4\beta\epsilon)^{(3j+1)/6} \Gamma\left(\frac{3j-1}{6}\right).$$

The comparison shows that

$$\lim_{q \rightarrow \infty} \sum_m \delta_m(q) = -\frac{3}{10} \pi p^{1/3} q^{5/3}.$$

It follows that the error in the second virial coefficient owing to a cut off  $q_c$  is approximately

$$\frac{3}{5} \pi\sigma^2 (4\beta\epsilon)^{1/6} \int_y^\infty x^{5/6} e^{-x} dx,$$

where

$$y = 4\beta\epsilon q_c^2/p^2.$$

With the de Boer-Michels parameters for helium of  $\sigma = 2.556 \text{ \AA}$ ,  $\epsilon/k = 10.22 \text{ K}$  the values of  $p^2$  for  $\text{He}^4$ ,  $\text{He}^3$  and the  $\text{He}^4$ - $\text{He}^3$  problem are 22.05, 16.61, and 18.95, respectively. With these values of  $p^2$  the average value of the error in the second virial coefficient due to a cut off  $q_c$  of 20 is negligible ( $\sim 10^{-4} \text{ \AA}^2$ ) for helium at 60 K, the maximum temperature which we considered.

The bound states of the Lennard-Jones potential are found by equating the logarithmic derivatives of the inside and outside radial solution at some cut off  $x_c$ . This yields the following equation which determines the characteristic values of  $q$  and the bound-state energies  $E_B = -4\epsilon q^2/p^2$ ,

$$\frac{R'_{m,q}(x_c)}{R_{m,q}(x_c)} = \frac{qK'_m(qx_c)}{K_m(qx_c)},$$

where  $K_m$  is the modified Bessel function of the second kind of order  $m$ . The radial cut off was chosen such that the first-order perturbation correction to any energy level due to the potential beyond the cut off was less than  $10^{-8}\epsilon$ . The radial

wave functions and the first derivatives were calculated from the Numerov process.

For the two-particle  $\text{He}^4$ ,  $\text{He}^3$ , and  $\text{He}^4\text{-He}^3$  problems, we find one bound state with  $m=0$ . The energies of this state are

TABLE III. Second virial coefficients for two-dimensional  $\text{He}^3$ .

$T$	$B$	$\beta \frac{dB}{d\beta}$	$\beta^2 \frac{d^2B}{d\beta^2}$
0.100 00	24.981 87	76.633 95	14.288 03
0.200 00	-9.735 68	28.112 49	23.752 79
0.400 00	-18.954 12	1.424 83	24.883 58
0.600 00	-17.714 66	-6.724 39	20.998 54
0.800 00	-15.290 34	-9.797 18	17.137 17
1.000 00	-12.959 03	-10.938 62	13.995 43
1.200 00	-10.930 06	-11.234 76	11.538 33
1.400 00	-9.202 25	-11.135 90	9.626 62
1.600 00	-7.732 54	-10.850 05	8.131 82
1.800 00	-6.475 45	-10.480 00	6.953 07
2.000 00	-5.391 92	-10.078 64	6.014 44
2.200 00	-4.450 36	-9.673 63	5.259 30
2.400 00	-3.625 66	-9.279 32	4.645 39
2.600 00	-2.897 91	-8.902 85	4.141 05
2.800 00	-2.251 29	-8.547 33	3.722 40
3.000 00	-1.673 09	-8.213 62	3.371 28
3.200 00	-1.153 07	-7.901 43	3.073 82
3.400 00	-0.682 90	-7.609 78	2.819 36
3.600 00	-0.255 74	-7.337 40	2.599 60
3.800 00	0.134 08	-7.082 89	2.408 08
4.000 00	0.491 26	-6.844 85	2.239 73
4.200 00	0.819 77	-6.621 94	2.090 55
4.400 00	1.122 95	-6.412 88	1.957 33
4.600 00	1.403 63	-6.216 52	1.837 52
4.800 00	1.664 27	-6.031 77	1.729 05
5.000 00	1.906 93	-5.857 65	1.630 26
6.000 00	2.906 57	-5.118 61	1.241 19
7.000 00	3.650 71	-4.543 90	0.963 78
8.000 00	4.226 30	-4.082 60	0.751 98
9.000 00	4.684 55	-3.702 82	0.583 08
10.000 00	5.057 70	-3.383 70	0.444 41
11.000 00	5.367 09	-3.111 06	0.328 11
12.000 00	5.627 43	-2.874 91	0.229 00
14.000 00	6.040 09	-2.484 96	0.068 74
16.000 00	6.350 93	-2.174 87	-0.055 40
18.000 00	6.591 98	-1.921 36	-0.154 49
20.000 00	6.783 14	-1.709 59	-0.235 43
22.000 00	6.937 42	-1.529 63	-0.302 78
24.000 00	7.063 70	-1.374 49	-0.359 69
26.000 00	7.168 27	-1.239 17	-0.408 38
28.000 00	7.255 64	-1.119 95	-0.450 49
30.000 00	7.329 23	-1.014 00	-0.487 24
32.000 00	7.391 59	-0.919 14	-0.519 59
34.000 00	7.444 70	-0.833 65	-0.548 25
36.000 00	7.490 12	-0.756 15	-0.573 81
38.000 00	7.529 09	-0.685 54	-0.596 73
40.000 00	7.562 58	-0.620 91	-0.617 38
45.000 00	7.627 35	-0.480 80	-0.660 98
50.000 00	7.671 82	-0.364 82	-0.695 84
55.000 00	7.701 89	-0.267 05	-0.724 53
60.000 00	7.721 44	-0.183 37	-0.749 26

TABLE IV. Second virial coefficients for two-dimensional  $\text{He}^4$ .

$T$	$B$	$\beta \frac{dB}{d\beta}$	$\beta^2 \frac{d^2B}{d\beta^2}$
0.100 00	-1134.809 84	-1761.561 88	-1195.242 76
0.200 00	-401.728 09	-584.425 58	-307.123 40
0.400 00	-150.066 39	-207.857 80	-97.017 88
0.600 00	-86.435 71	-115.388 14	-49.767 72
0.800 00	-59.171 63	-76.984 87	-28.983 53
1.000 00	-44.349 07	-57.030 24	-17.619 25
1.200 00	-35.081 15	-45.200 74	-10.822 29
1.400 00	-28.728 71	-37.524 06	-6.569 85
1.600 00	-24.085 82	-32.195 23	-3.840 03
1.800 00	-20.529 89	-28.297 11	-2.060 59
2.000 00	-17.708 96	-25.323 87	-0.891 07
2.200 00	-15.409 48	-22.978 15	-0.120 77
2.400 00	-13.494 40	-21.075 78	0.384 37
2.600 00	-11.871 61	-19.497 64	0.711 46
2.800 00	-10.476 81	-18.163 73	0.918 01
3.000 00	-9.263 65	-17.018 54	1.042 50
3.200 00	-8.197 82	-16.022 42	1.110 96
3.400 00	-7.253 30	-15.146 31	1.141 16
3.600 00	-6.410 00	-14.368 46	1.145 29
3.800 00	-5.652 13	-13.672 22	1.131 82
4.000 00	-4.967 06	-13.044 60	1.106 60
4.200 00	-4.344 61	-12.475 37	1.073 71
4.400 00	-3.776 41	-11.956 27	1.036 01
4.600 00	-3.255 58	-11.480 60	0.995 49
4.800 00	-2.776 34	-11.042 85	0.953 52
5.000 00	-2.333 86	-10.638 43	0.911 07
6.000 00	-0.547 58	-8.999 96	0.708 22
7.000 00	0.745 46	-7.802 67	0.534 87
8.000 00	1.724 94	-6.884 92	0.390 79
9.000 00	2.492 26	-6.156 47	0.270 46
10.000 00	3.109 17	-5.562 65	0.168 79
11.000 00	3.615 48	-5.068 24	0.081 83
12.000 00	4.038 04	-4.649 50	0.006 62
14.000 00	4.701 85	-3.977 03	-0.116 96
16.000 00	5.197 69	-3.458 97	-0.214 28
18.000 00	5.580 42	-3.046 32	-0.292 91
20.000 00	5.883 36	-2.709 06	-0.357 75
22.000 00	6.127 98	-2.427 71	-0.412 12
24.000 00	6.328 71	-2.189 08	-0.458 35
26.000 00	6.495 63	-1.983 87	-0.498 11
28.000 00	6.635 97	-1.805 32	-0.532 65
30.000 00	6.755 06	-1.648 43	-0.562 92
32.000 00	6.856 93	-1.509 37	-0.589 64
34.000 00	6.944 64	-1.385 18	-0.613 40
36.000 00	7.020 60	-1.273 55	-0.634 66
38.000 00	7.086 70	-1.172 61	-0.653 83
40.000 00	7.144 48	-1.080 84	-0.671 25
45.000 00	7.260 01	-0.883 99	-0.709 32
50.000 00	7.344 54	-0.722 93	-0.743 97
55.000 00	7.406 94	-0.587 91	-0.781 75
60.000 00	7.453 00	-0.471 84	-0.830 48

$$\begin{aligned}
E_B/k &= -4.63 \times 10^{-7} \text{ K} \quad (\text{He}^3), \\
&= -2.36 \times 10^{-2} \text{ K} \quad (\text{He}^4), \\
&= -1.45 \times 10^{-3} \text{ K} \quad (\text{He}^3\text{-He}^4).
\end{aligned}$$

The bound states for  $\text{He}^3$  and  $\text{He}^4$  have been calculated by Bagchi<sup>26</sup> who finds  $-1.8 \times 10^{-7}$  K for  $\text{He}^3$  and  $-2.57 \times 10^{-2}$  K for  $\text{He}^4$ . In the calculation of the second virial coefficient, we employed the binding energies calculated by us.

Our results for the second virial coefficients are presented in Tables III–V. Those for the  $\text{He}^3$  and  $\text{He}^4$  are shown in Fig. 6 together with the classical result. The general features of all three results are as expected. At high temperatures, the virial coefficient is positive due to the effect of the hard core. As the temperature is lowered, the attractive part of the potential has a greater effect and causes  $B$  to become negative. By calculating  $B$  for a hypothetical spinless boson of the mass of  $\text{He}^3$ , we have determined that above 3 K the difference in the  $\text{He}^3$  and  $\text{He}^4$  virial coefficients shown in Fig. 6 is due to the difference in mass. The effects of spin and statistics, given in the quantity

$$B_B(M_3) - B_F^{(1/2)}(M_3) = \frac{3}{4}[B_B(M_3) - B_F(M_3)],$$

are significant only below this temperature. The relevance of this statement to the magnetic susceptibility of  $\text{He}^3$  will be explored later.

Our results for the quantity of interest in the specific heat

$$-\beta^2 \frac{d^2 B}{d\beta^2} \approx \frac{C/Nk - 1}{n}$$

are given in Tables III and IV and shown in Fig. 7. We immediately see several points of qualitative agreement with the experimental data. First, at 4 K the predicted specific heat is less than unity. Second, for equal densities the specific heat of  $\text{He}^3$  is predicted to deviate more from unity than that of  $\text{He}^4$ . Third, and most important, the  $\text{He}^4$  specific heat increases with decreasing temperature crossing unity at 2.2 K, while the  $\text{He}^3$  specific heat decreases with temperature. It is of interest to investigate the origins of this behavior.

We begin by noting that Eq. (3.20) indicates that the low-temperature behavior of  $B$  is dominated by those phase shifts which are significant at small  $k$ . In general, these are the phase shifts with small values of  $|m|$ . Thus the boson virial coefficient which depends only on even values of  $m$  is dominated by  $\delta_0$  at low temperatures. This phase shift is dominated by the hard-core interaction since there is no angular momentum. It is not surprising then that the  $\text{He}^4$  signal increases with decreasing temperature as this was precisely the behavior found in the hard-core interaction. The

interesting question then is why the  $\text{He}^3$  specific heat falls. Clearly it must be due to the attractive part of the interaction as we have seen that the hard core also causes the fermions specific heat to rise.

TABLE V. The quantity  $B_{34}$  needed for the second virial coefficients for two-dimensional  $\text{He}^3\text{-He}^4$  mixture.

$T$	$B$	$\beta \frac{dB}{d\beta}$	$\beta^2 \frac{d^2 B}{d\beta^2}$
0.100 00	-245.747 79	-257.244 32	-56.056 06
0.200 00	-123.618 01	-116.821 97	-5.721 29
0.400 00	-64.986 74	-60.310 21	7.838 80
0.600 00	-44.293 82	-42.941 40	8.073 80
0.800 00	-33.265 11	-34.108 10	7.117 23
1.000 00	-26.285 78	-28.616 86	6.214 23
1.200 00	-21.422 94	-24.819 76	5.481 39
1.400 00	-17.817 64	-22.013 54	4.891 76
1.600 00	-15.025 62	-19.842 23	4.409 71
1.800 00	-12.792 42	-18.104 55	4.008 10
2.000 00	-10.961 10	-16.677 44	3.667 71
2.200 00	-9.429 26	-15.481 11	3.374 95
2.400 00	-8.127 08	-14.461 41	3.120 01
2.600 00	-7.005 17	-13.580 18	2.895 65
2.800 00	-6.027 57	-12.809 75	2.696 43
3.000 00	-5.167 46	-12.129 48	2.518 13
3.200 00	-4.404 34	-11.523 67	2.357 47
3.400 00	-3.722 32	-10.980 13	2.211 83
3.600 00	-3.108 84	-10.489 26	2.079 10
3.800 00	-2.553 85	-10.043 37	1.957 57
4.000 00	-2.049 20	-9.636 25	1.845 80
4.200 00	-1.588 21	-9.262 79	1.742 61
4.400 00	-1.165 35	-8.918 76	1.647 02
4.600 00	-0.776 01	-8.600 65	1.558 17
4.800 00	-0.416 28	-8.305 46	1.475 35
5.000 00	-0.082 87	-8.030 69	1.397 94
6.000 00	1.275 71	-6.897 03	1.075 55
7.000 00	2.272 19	-6.047 19	0.831 13
8.000 00	3.034 61	-5.382 72	0.638 81
9.000 00	3.636 60	-4.846 68	0.483 19
10.000 00	4.123 62	-4.403 70	0.354 47
11.000 00	4.525 36	-4.030 53	0.246 13
12.000 00	4.862 02	-3.711 21	0.153 60
14.000 00	5.393 34	-3.191 80	0.003 75
16.000 00	5.792 01	-2.785 74	-0.112 47
18.000 00	6.100 57	-2.458 38	-0.205 29
20.000 00	6.345 17	-2.188 10	-0.281 14
22.000 00	6.542 75	-1.960 67	-0.344 27
24.000 00	6.704 81	-1.766 30	-0.397 62
26.000 00	6.839 39	-1.598 05	-0.443 27
28.000 00	6.952 31	-1.450 80	-0.482 75
30.000 00	7.047 88	-1.320 72	-0.517 22
32.000 00	7.129 35	-1.204 88	-0.547 55
34.000 00	7.199 22	-1.100 99	-0.574 42
36.000 00	7.259 45	-1.007 24	-0.598 38
38.000 00	7.311 60	-0.922 15	-0.619 87
40.000 00	7.356 89	-0.844 56	-0.639 24
45.000 00	7.446 37	-0.677 33	-0.680 28
50.000 00	7.510 40	-0.539 85	-0.713 66
55.000 00	7.556 29	-0.424 55	-0.742 79
60.000 00	7.588 91	-0.326 09	-0.771 40

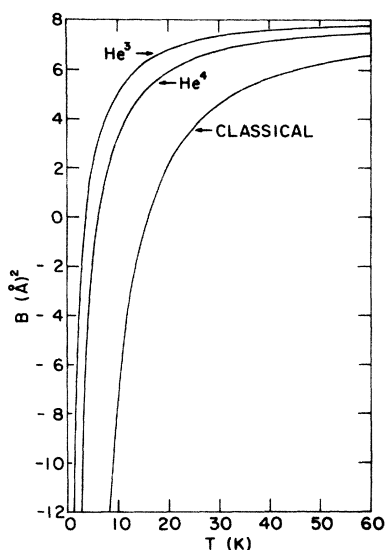


FIG. 6. Second virial coefficients for 2D systems of  $\text{He}^3$  and  $\text{He}^4$ .

At low temperatures, the most important contributions to the  $\text{He}^3$  virial coefficient will come from  $\delta_0$  which is weighted by a factor of  $\frac{1}{4}$  and reflects the hard core, and  $\delta_1$  and  $\delta_{-1}$  which give identical contributions and which are each weighted by a factor of  $\frac{3}{4}$ . The phase shift  $\delta_1$  is dominated by collision which occur with an average impact parameter  $b$  which is approximately

$$b \approx \hbar / \mu v,$$

where  $v$  is an average velocity. With  $\mu v^2 \sim kT$  we find  $b \sim \lambda$ . The thermal wavelength of  $\text{He}^3$  is  $10/\sqrt{T}$  in angstroms so that at 4 K,  $\lambda$  is 5 Å. Since the minimum of the Lennard-Jones potential occurs at

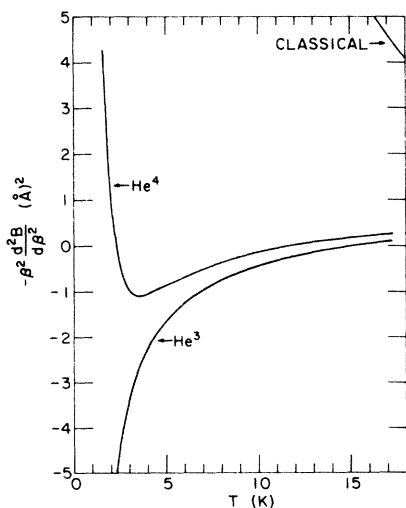


FIG. 7. Deviation of the specific heat from unity per unit density for 2D  $\text{He}^3$  and  $\text{He}^4$  systems.

2.87 Å, these collisions are dominated by the attractive part of this interaction which strengthens our suspicion that it is the attraction which causes the specific heat to fall. To verify this, we have calculated the contribution to the  $\text{He}^3$  virial coefficient from  $\delta_0$ ,  $\delta_{\pm 1}$  up to  $\delta_{\pm 4}$ . These contributions are shown in Fig. 8. It is to be noted that the curve labeled  $\delta_1$  is the contribution from both  $\delta_1$  and  $\delta_{-1}$ , and similarly for higher  $m$  values. It is seen that the  $\delta_0$  contribution by itself would cause the specific heat to rise but that the major contribution comes from  $\delta_1$  which reflects the attraction. We conclude therefore that the  $\text{He}^4$  specific heat rises with decreasing temperature while the  $\text{He}^3$  specific heat falls due to the fact that the difference in statistics causes the different isotopes to see different parts of the interaction; the  $\text{He}^4$  signal is dominated by the hard core while the  $\text{He}^3$  signal is dominated by the attraction.

The dominance of the attractive part of the interaction cannot be maintained indefinitely with decreasing temperature. As noted earlier, collisions characterized by  $|m|$  equal to unity have an average impact parameter of order  $\lambda$ . As the temperature decreases,  $\lambda$  increases and the impact parameter greatly exceeds the range of the attraction. Thus the contribution of  $\delta_1$  must fall and that of  $\delta_0$  must dominate at sufficiently low temperature. From Fig. 8 it can be seen that this occurs at a temperature of about 0.3 K. This leads us to suspect that this occurrence may be responsible for the shoulder observed in the low-temperature  $\text{He}^3$  specific heats.

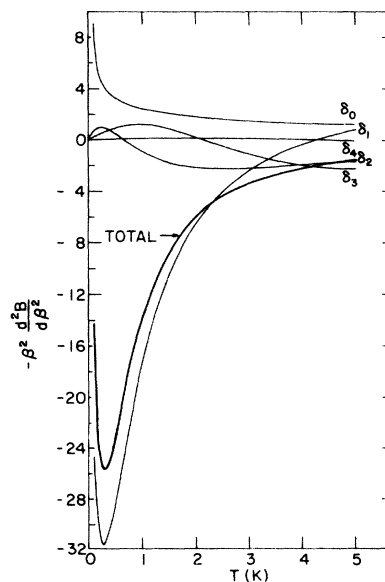


FIG. 8. Contribution from different angular-momentum states to the  $\text{He}^3$  specific-heat deviation per unit density.

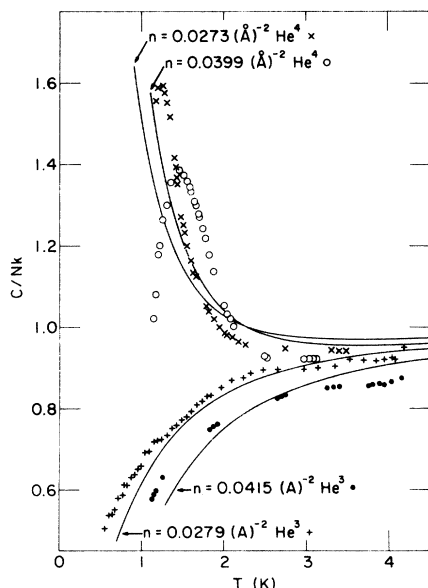


FIG. 9. Comparison of calculated and observed specific heats for two densities of He<sup>3</sup> and He<sup>4</sup>.

#### V. COMPARISON WITH EXPERIMENT

Figure 9 shows a comparison between our calculated results and the experimental data shown previously in Figs. 1 and 3. In addition to the points of qualitative agreement noted in the Sec. IV, Fig. 9 shows that the predicted deviations from unity increase with increasing density as is observed. In addition, as a consequence of the vanishing of  $-\beta^2 d^2B/d\beta^2$  at 2.2 K, all He<sup>4</sup> specific heats are predicted to cross one another there at a value of  $C/Nk$  equal to 1. The experimental He<sup>4</sup> signals do

cross one another at this temperature but at a value of  $C/Nk$  somewhat less than unity. Figure 9 also shows that the quantitative agreement with the experimental data is rather good, particularly for the He<sup>3</sup>. In fact, the agreement down to temperatures of the order of 1 K is initially disturbing as the values of  $n\lambda^2$  for the He<sup>3</sup> densities shown are 2.82 and 4.19 at 1 K and it might be surmised that the truncation of the expansion for the specific heat is invalid. To determine the range of temperature and densities for which the truncated series remains a good approximation, we have employed the following procedure. We note that, if the contributions of the third virial coefficient to the specific heat can be ignored then

$$(C/Nk - 1)/n = -\beta^2 \frac{d^2B}{d\beta^2}.$$

The right-hand side is a function of temperature only. Therefore if the experimental data are plotted as on the left-hand side and the truncated series is adequate, then the data for different densities will fall on a universal curve depending only on temperature. Data from He<sup>3</sup> samples at seven different densities are plotted in this manner in Fig. 10 and compared with our theoretical results. The experimental uncertainty in the data shown can be inferred from the estimated 2% uncertainty in  $C/Nk$ . It can be seen that down to about 0.6 K a virial description containing only the contribution of the second virial coefficient is completely adequate for the specific heat of the He<sup>3</sup> samples shown. The agreement with the calculated values is very good. Below 0.6 K contributions from higher coefficients can be seen. We shall discuss this

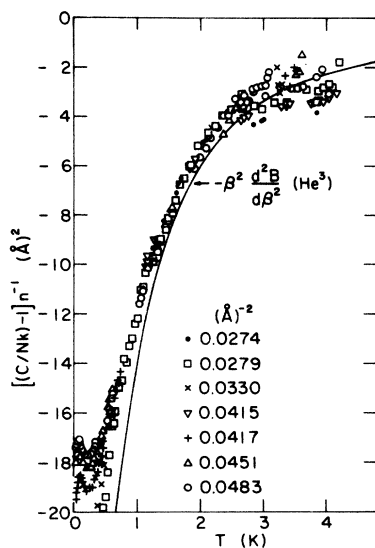


FIG. 10. Comparison of calculated and observed specific-heat deviation per unit density for He<sup>3</sup>.

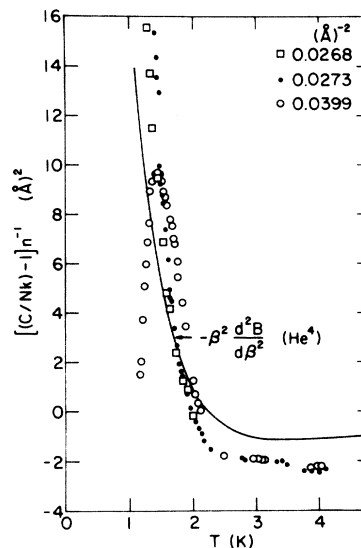


FIG. 11. Comparison of calculated and observed specific-heat deviation per unit density for He<sup>4</sup>.

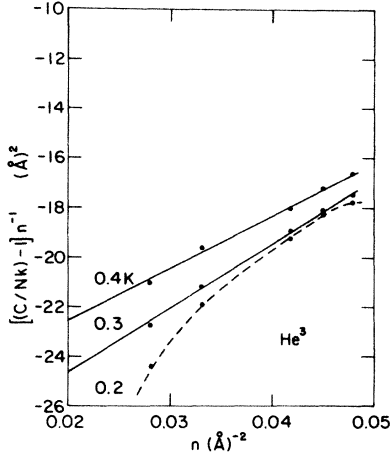


FIG. 12. Observed specific heat deviation per unit density plotted versus density.

region below.

A similar plot of data from He<sup>4</sup> samples at three different densities is shown in Fig. 11. This figure shows that the truncated virial expansion of the specific heat is completely adequate at these densities down to 2 K. The agreement with the calculated results is good.

We next examine the low-temperature He<sup>3</sup> heat capacity. We note that if the contributions to *C* from the third virial coefficient are included that, from Eq. (3.8),

$$(C/Nk - 1)/n = -\beta^2 \frac{d^2 B}{d\beta^2} - \frac{1}{2} n\beta^2 \frac{d^2 B_3}{d\beta^2}.$$

If the data in the form of the left-hand side are plotted versus density at a given temperature, a

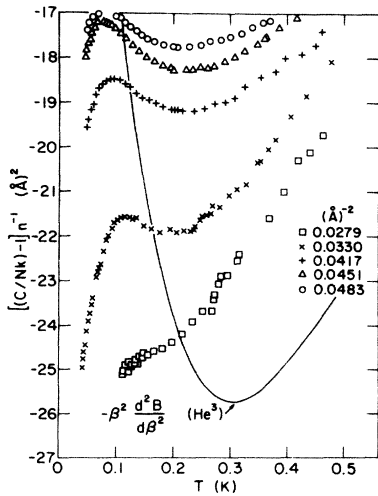


FIG. 13. Comparison of calculated and observed specific-heat deviation per unit density for He<sup>3</sup> at low temperatures.

straight line will result provided that this description is adequate. Such a plot is shown for the He<sup>3</sup> data in Fig. 12. It can be seen that a virial description which includes contributions from the third virial coefficient is completely satisfactory at these densities down to 0.3 K. We note in passing that the value of  $\beta^2 d^2 B_3/d\beta^2$  obtained from the slope of the straight line in Fig. 12 is  $-400 \text{ \AA}^4$  at 0.4 K, which is far from the value of this quantity for an ideal Fermi gas. That value obtained from  $B_3^0 = +\frac{1}{128} \lambda^4$ , is  $+996 \text{ \AA}^4$ .

Figure 13 shows the low-temperature He<sup>3</sup> data plotted as in Fig. 11 together with the calculated contribution from the second virial coefficient. From the fact that the data do not lie on a universal curve, it is clear that higher virial coefficients are contributing. We know from Fig. 12 that at 0.2 K at least the contribution from the third and fourth virial coefficients can not be ignored. It might be argued, therefore, that the shoulder indicates a collective effect, such as liquefaction, taking place in the He<sup>3</sup>. That this shoulder also occurs in the bulk liquid mitigates this point of view. We believe that the fact that the shoulder appears at just the temperature at which the contribution from the second virial coefficient is rising indicates that the signal is due to the effect of the hard core in precisely the same way in which the rise of the He<sup>4</sup> signal can be attributed to it. Thus, the shoulder in the He<sup>3</sup> signal and the rise in the He<sup>4</sup> signal have precisely the same origin. They occur at different temperatures due to the difference in statistics.

### VI. LIQUEFACTION

We have argued that a system of hard discs would exhibit a rounded peak in its specific heat

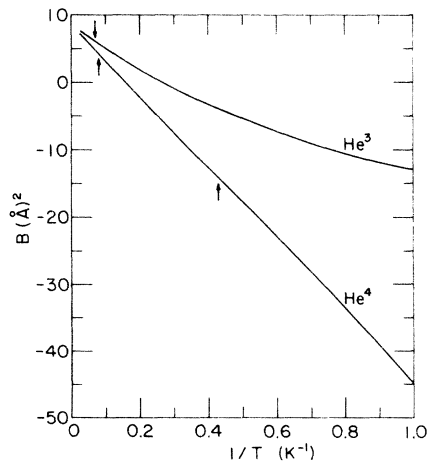


FIG. 14. Second virial coefficient of 2D systems of He<sup>3</sup> and He<sup>4</sup> plotted versus inverse temperature.

due to the interactions without a phase transition occurring. We have also argued that the rise in the He<sup>4</sup> specific heat with decreasing temperature is also due to the two-body interaction. We now address ourselves to the question of whether the low-temperature fall of the He<sup>4</sup> specific heat is due to higher virial coefficients as in the hard-disc systems or to liquefaction in the He<sup>4</sup> as has been suggested by Novaco.<sup>11</sup> There are several ways to examine this question.

The method we choose is to fit the calculated second virial coefficient to the form of a van der Waals second virial coefficient

$$B(\beta) = b - a\beta.$$

The values of  $a$  and  $b$  so obtained may be substituted into the expression for the critical temperature and density of a van der Waal gas

$$T_c = 8a/27b, \quad n_c = 1/3b.$$

Such a procedure for the bulk system<sup>27</sup> yields  $T_c = 7.2$  K,  $n_c = 0.0215$  cm<sup>3</sup>/mole for He<sup>4</sup> compared to the experimental values of 5.2 K and 0.0169 cm<sup>3</sup>/mole. The predictions for He<sup>3</sup> are 5.7 K, 0.0215 cm<sup>3</sup>/mole compared to the experimental values of 3.3 K and 0.0139 cm<sup>3</sup>/mole.

Our calculated values of  $B$  for He<sup>4</sup> and He<sup>3</sup> plotted vs  $\beta$  are shown in Fig. 14. It is clear that the 2D He<sup>3</sup> virial coefficient does not have the van der Waal form. On the other hand, the He<sup>4</sup> virial coefficient can be remarkably well fit by a straight line from 1 to 10 K in spite of the fact that there are two points of inflection shown by arrows in the figure. The resulting prediction for  $T_c$  and  $n_c$  are 1.93 K and 0.0437 Å<sup>-2</sup>. If these results are adjusted downwards by the ratio of the observed bulk properties to the predicted bulk properties of He<sup>4</sup>, we obtain a  $T_c$  of 1.4 K and  $n_c$  of 0.034 Å<sup>-2</sup>. A glance at Fig. 9 shows that the He<sup>4</sup> peaks in samples of density near  $n_c$  do occur very near 1.4 K. We therefore believe that a liquid-gas transition occurs in the He<sup>4</sup> system.

## VII. SUMMARY

The study of the second virial coefficient has provided many clues to the interpretation of the specific-heat measurements from adsorbed helium films and it is perhaps wise at this point to summarize our interpretation of these signals.

In the He<sup>3</sup> system at 4 K the fact that the specific heat is appreciably less than unity is due simply to the interactions within the system. Effects of spin and statistics are unimportant but the remaining quantum effects are still appreciable as the classical signal is always greater than unity. As the temperature is lowered, the effect of spin and

statistics is to cause the signal to be dominated by those collisions which are most strongly affected by the attractive part of the interaction. As a result the signal falls. As the temperature continues to fall, the effect of these attractive interactions becomes progressively weaker until, at 0.3 K, the collision in the  $m$  equal to zero state, affected by the hard core, begin to dominate the signal. This causes the signal to rise, producing a shoulder. Although it can be argued that the subsequent fall of the signal to zero is due to a cooperative transition, we feel there is little compelling evidence for this at this time and attribute the fall to higher-order terms in the virial series as in the hard-disc gas. The striking agreement of the experimental data with our results which posit a featureless passive substrate indicates that the substrate potential has little effect on the specific heat. It also indicates that the substrate is either very uniform or that inhomogeneities have little effect on the signal in the density range studied.

In the He<sup>4</sup> system the signal at 4 K is again less than unity for the same reasons as in the He<sup>3</sup> case. As the temperature is lowered, the effect of statistics is to cause the signal to be dominated by collisions with  $m$  equal to zero which are affected by the hard core. As a result, the signal rises. As the temperature is lowered still further to about 1 K, a gas-liquid phase boundary is encountered and the system undergoes a phase separation. This is precisely the behavior expected in experiments on low-density bulk helium vapor. On encountering the phase boundary, one expects to see in general a discontinuity in the specific-heat signal instead of the rounded peak observed. The rounding of the peak has been attributed by Novaco<sup>11</sup> to inhomogeneities. It could also be due to a lack of equilibrium in the sample. This is easily understood when it is recalled that there is no external force which tends to separate the 2D liquid from the vapor. Consequently, equilibrium may take a very long time to achieve.<sup>28</sup> Below the transition, the signal is simply that from a two-phase 2D liquid-gas system. The agreement between the data and our calculated results, while not as striking as in the He<sup>3</sup> case, is still quite good. Whether the differences are due to the use of the Lennard-Jones potential instead of a more accurate model potential or reflect contributions from the substrate is a question we shall examine in a subsequent note.

## VIII. MAGNETIC SUSCEPTIBILITY

We conclude this paper with an additional piece of information that can be gleaned from the second virial coefficients, the zero-field magnetic suscep-

tibility per particle of 2D He<sup>3</sup> films. It is shown in the Appendix that this quantity has the virial expansion

$$\chi(\beta) = \chi_0(\beta) \left\{ 1 + \frac{1}{2} n [B_B(\beta) - B_F(\beta)] + O(n^2) \right\},$$

where  $\chi_0$  is the Curie susceptibility, and  $B_B$ ,  $B_F$  are the second virial coefficients of spinless bosons or fermions of He<sup>3</sup> mass. The above expression indicates that in a density and temperature region in which higher virial coefficient can be ignored

$$(\chi/\chi_0 - 1)n^{-1} = \frac{1}{2}[B_B(\beta) - B_F(\beta)], \quad (8.1)$$

so that the data plotted as on the left should fall on a common function of temperature. Our results for this function are shown in Fig. 15 together with its ideal-quantum-gas limit of  $-\frac{1}{2}\lambda^2$ . It is immediately seen that the deviations from the Curie susceptibility are predicted to be much less than those occurring in the ideal gas. This behavior is precisely what is observed in the bulk vapor<sup>29</sup> and in He<sup>3</sup> trapped in surface states.<sup>30</sup> The reason for this behavior can be seen from the following argument.

If the He<sup>3</sup> atoms were distinguishable (Boltzman) particles then the scattering in any angular-momentum state could occur with any relative spin orientation. Thus the spins would be completely unaffected by the spin-independent interaction and the susceptibility would be that of independent spins  $\chi_0$ . It is only through the requirement of statistics that scattering in an even  $m$  state be singlet and that in an odd  $m$  state be triplet that the interaction affects the susceptibility. This is the reason that Eq. (8.1) depends on the difference between the spinless-boson and -fermion coefficients. For the effects of statistics to be important, the particles must be within a certain length, which is on the order of a thermal wavelength, of one another. Above a temperature for which this length is smaller than the hard-core diameter, the statistics can play no role and the susceptibility must take the Curie value. At this same temperature the difference in the He<sup>4</sup> and He<sup>3</sup> virial coefficients is due solely to their mass difference. As noted earlier and seen from Fig. 15, this temperature is approximately 3 K.

In summary, the hard-core repulsions tend to decrease the effects of statistics. The ideal-gas model overemphasizes the role of statistics and thus gives a larger deviation from the Curie value. The above argument is probably also applicable to bulk liquid He<sup>3</sup> in the temperature region for which it is not a Landau Fermi liquid. It is well known that in this range the susceptibility is much nearer the Curie value than an ideal-gas model predicts.

A fruitful approach for the liquid would then appear to be to expand the susceptibility about the Curie value in a power series in which the effect of statistics is the small parameter. Such an approach has recently been taken by Sykes<sup>31</sup> with encouraging results.

#### ACKNOWLEDGMENTS

We are grateful to M. Bretz, J. G. Dash, and O. E. Vilches for their sustained interest in and encouragement of this work and to Sir R. E. Peierls for a seminal conversation.

#### APPENDIX

We outline below the derivation of the virial expansion for the zero-field magnetic susceptibility of a spin- $\frac{1}{2}$  fermion system. An alternative derivation can be found in Ref. 29.

Let  $H_0$  be the spin-independent part of the two-particle Hamiltonian and define the thermodynamic potential  $\Omega(A, \beta, H)$  according to

$$e^{\beta A \Omega} = \text{Tr} e^{-\beta(H_0 - \mu N - M \mathcal{H})},$$

where  $\mathcal{H}$  is a magnetic field and  $M$  is the magnetization of the  $N$ -particle system

$$M = \gamma \sum_i^N \sigma_i^z,$$

with  $\gamma$  an uninteresting constant. The  $l$ th cluster integral for this system will be denoted  $c_l^F$  and is

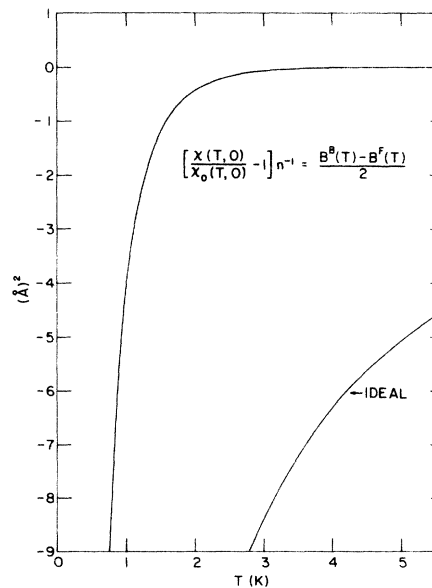


FIG. 15. Predicted deviation of the 2D He<sup>3</sup> zero-field magnetic susceptibility from the Curie value per unit density.

defined by the expansion

$$\beta\Omega(\beta, z, A, \mathcal{H}) = \sum_{l=1}^{\infty} z^l c_l^F(A, \beta, \mathcal{H}).$$

It follows that the density, magnetization per unit area, and susceptibility per unit area have the following cluster expansions:

$$n = \sum_{l=1}^{\infty} l c_l^F z^l, \quad (A1)$$

$$M/A = \beta^{-1} \sum_{l=1}^{\infty} z^l \frac{\partial c_l^F}{\partial \mathcal{H}},$$

$$\chi_A = \beta^{-1} \sum_{l=1}^{\infty} z^l \frac{\partial^2 c_l^F}{\partial \mathcal{H}^2}. \quad (A2)$$

Upon solving Eq. (A1) for  $z$  in terms of  $n$  and substituting in Eq. (A2) one obtains

$$\beta\chi_A = \frac{n}{c_1^F} \frac{\partial^2 c_1^F}{\partial \mathcal{H}^2} + n^2 \frac{c_2^F}{(c_1^F)^2} \left( \frac{1}{c_2^F} \frac{\partial^2 c_2^F}{\partial \mathcal{H}^2} - \frac{2}{c_1^F} \frac{\partial^2 c_1^F}{\partial \mathcal{H}^2} \right) + O(n^3). \quad (A3)$$

In a manner completely analogous to that discussed in Sec. III, the cluster integrals  $c_1^F$  and  $c_2^F$  may be expressed in terms of the one- and two-particle partition functions of spin- $\frac{1}{2}$  fermions. Because of the form of the Hamiltonian  $H_0 - M\mathcal{H}$ , these partition functions are products of spatial and spin factors. The spatial factors are simply  $Z_1$ ,  $Z_2^B$ , or  $Z_2^F$ , the one or two particle partition functions of spinless bosons or fermions. One finds

$$c_1^F(\mathcal{H}) = c_1(\mathcal{H}) = 2Z_1/A,$$

which is independent of statistics, and

$$c_2^F(\mathcal{H}) = A^{-1} [Z_2^F (e^{2\beta\gamma\mathcal{H}} + 1 + e^{-2\beta\gamma\mathcal{H}}) + Z_2^B - 2Z_1^2 \cosh^2 \beta\gamma\mathcal{H}].$$

The appropriate derivatives can now be taken and substituted into Eq. (A3). In the limit of vanishing magnetic field, one finds the following simple relationships between  $c_1(0)$ ,  $c_2^F(0)$ , and the first or second cluster integrals of spinless-boson or -fermion systems  $b_1$ ,  $b_2^B$ ,  $b_2^F$ :

$$c_1(0) = 2b_1,$$

$$c_2^F(0) = 3b_2^F + b_2^B,$$

$$\frac{\partial^2 c_1(0)}{\partial \mathcal{H}^2} = 2\beta^2 \gamma^2 b_1,$$

$$\frac{\partial^2 c_2^F(0)}{\partial \mathcal{H}^2} = 8\beta^2 \gamma^2 b_2^F.$$

Lastly we use the fact that the second virial coefficient of spinless-boson system can be expressed in terms of the cluster integrals as discussed in Sec. III and has the form  $B^B = -b_2^B/b_1^2$ . Similarly, for a spinless-fermion system,  $B^F = -b_2^F/b_1^2$ . From Eq. (A3) one then obtains, for the zero-field magnetic susceptibility per particle  $\chi = \chi_A/n$ , the result

$$\chi = \chi_0 [1 + \frac{1}{2} n(B_B - B_F) + O(n^2)],$$

where  $\chi_0$  is the Curie susceptibility  $\beta\gamma^2$ .

\*Work supported in part by the National Science Foundation.

†Present address: Department of Physics, U.S. Naval Academy, Annapolis, Md. 21402.

<sup>1</sup>A comprehensive review of the experimental data and an easy access to the literature are provided by M. Bretz, J. G. Dash, D. C. Hickernell, E. O. McLean, and O. E. Vilches, Phys. Rev. A **8**, 1589 (1973).

<sup>2</sup>J. M. Kosterlitz and D. J. Thouless, J. Phys. C **6**, 1181 (1973).

<sup>3</sup>V. L. Berezinskii, Zh. Eksp. Teor. Fiz. **61**, 1144 (1971) [Sov. Phys.—JETP **34**, 610 (1972)].

<sup>4</sup>M. Bretz, in *Proceedings of the Thirteenth International Conference on Low Temperature Physics, Colo.*, 1972, edited by R. H. Kropschot and R. O. Timmerhaus (University of Colorado Press, Boulder, Colo., 1973); Phys. Rev. Lett. **31**, 1447 (1973).

<sup>5</sup>S. C. Ying, Phys. Rev. B **3**, 4160 (1971); C. E. Campbell and M. Schick, Phys. Rev. A **5**, 1919 (1972).

<sup>6</sup>R. L. Elgin, Ph.D. thesis (California Institute of Technology, 1973) (unpublished).

<sup>7</sup>M. Bretz and J. G. Dash, Phys. Rev. Lett. **26**, 963 (1971).

<sup>8</sup>D. C. Hickernell, E. O. McLean, and O. E. Vilches, Phys. Rev. Lett. **28**, 789 (1972).

<sup>9</sup>L. Goldstein, Phys. Rev. **96**, 1455 (1954).

<sup>10</sup>C. E. Campbell, J. G. Dash, and M. Schick, Phys. Rev. Lett. **26**, 966 (1971); A. Widom and J. B. Sokoloff, Phys. Rev. A **5**, 475 (1972).

<sup>11</sup>A. D. Novaco, J. Low Temp. Phys. **9**, 457 (1972).

<sup>12</sup>D. E. Hagen, A. D. Novaco, and F. J. Milford, in *Proceedings of the Symposium on Adsorption-Desorption Phenomena, Florence, Italy, 1971* (Academic, New York, 1972).

<sup>13</sup>R. M. May, Phys. Rev. **135**, A1515 (1964).

<sup>14</sup>See J. E. Mayer and M. G. Mayer, *Statistical Mechanics* (Wiley, New York, 1940).

<sup>15</sup>B. Kahn and G. E. Uhlenbeck, Physica **5**, 399 (1938).

<sup>16</sup>J. Kilpatrick, J. Chem. Phys. **21**, 274 (1953).

<sup>17</sup>A convenient access to the literature concerning the third virial coefficient is provided by S. Y. Larsen and P. L. Mascheroni, Phys. Rev. A **2**, 1018 (1970).

<sup>18</sup>This argument is not rigorous however. The proper procedure is discussed by N. Fukuda and R. G. Newton [Phys. Rev. **103**, 1558 (1956)].

<sup>19</sup>F. Calogero, *Variable Phase Approach to Potential*

- Scattering* (Academic, New York, 1967).
- <sup>20</sup>R. L. Siddon, Ph.D. thesis (University of Washington, 1973) (unpublished).
- <sup>21</sup>G. N. Watson, *Theory of Bessel Functions* (Cambridge U. P., Cambridge, England, 1952).
- <sup>22</sup>W. A. Steele and E. J. Derderian, in Ref. 12.
- <sup>23</sup>M. E. Boyd, S. Y. Larsen, and J. E. Kilpatrick, *J. Chem. Phys.* 50, 4034 (1969).
- <sup>24</sup>*A posteriori* we find that the approximations of Ref. 22 are good to within 5% at 50 K but differ by 20% at 15 K from our exact results.
- <sup>25</sup>P. C. Chow, *Am. J. Phys.* 40, 730 (1972).
- <sup>26</sup>A. Bagchi, *Phys. Rev. A* 3, 1133 (1971).
- <sup>27</sup>We have used for this analysis the virial coefficients calculated by J. E. Kilpatrick, W. E. Keller, E. F. Hammel, and N. Metropolis [*Phys. Rev.* 94, 1103 (1954)].
- <sup>28</sup>This mechanism was suggested to us by J. G. Dash.
- <sup>29</sup>J. E. Opfer, K. Luszczynski, and R. E. Norberg, *Phys. Rev.* 140, A100 (1965).
- <sup>30</sup>D. F. Brewer, D. J. Creswell, and A. L. Thomson, in Ref. 4.
- <sup>31</sup>J. Sykes (private communication).